J Physiol Sci (2014) 64:421–431
DOI 10.1007/s12576-014-0337-4

ORIGINAL PAPER

Ex vivo cultured neuronal networks emit in vivo-like spontaneous activity

Kazuki Okamoto · Tomoe Ishikawa · Reimi Abe · Daisuke Ishikawa · Chiaki Kobayashi · Mika Mizunuma · Hiroaki Norimoto · Norio Matsuki · Yuji Ikegaya

Received: 10 July 2014 / Accepted: 27 August 2014 / Published online: 11 September 2014

Abstract Spontaneous neuronal activity is present in virtually all brain regions, but neither its function nor spatiotemporal patterns are fully understood. Ex vivo organotypic slice cultures may offer an opportunity to investigate some aspects of spontaneous activity, because they self-restore their networks that collapsed during slicing procedures. In hippocampal networks, we compared the levels and patterns of in vivo spontaneous activity to those in acute and cultured slices. We found that the firing rates and excitatory synaptic activity in the in vivo hippocampus are more similar to those in slice cultures compared to acute slices. The soft confidence-weighted algorithm, a machine learning technique without human bias, also revealed that hippocampal slice cultures resemble the in vivo hippocampus in terms of the overall tendency of the parameters of spontaneous activity.

Keywords Spontaneous activity · Slice culture · Machine learning algorism · Soft confidence-weighted learning

K. Okamoto and T. Ishikawa contributed equally to the present work.

K. Okamoto · T. Ishikawa · R. Abe · D. Ishikawa · C. Kobayashi · M. Mizunuma · H. Norimoto · N. Matsuki · Y. Ikegaya (✉)
Laboratory of Chemical Pharmacology, Graduate School of Pharmaceutical Sciences, University of Tokyo, 7-3-1 Hongo, Bunkyo-ku, Tokyo 113-0033, Japan
e-mail: ikegaya@mol.f.u-tokyo.ac.jp

Y. Ikegaya
Center for Information and Neural Networks, Suita City, Osaka 565-0871, Japan

Introduction

The neuronal network maintains ongoing activity spontaneously even in the absence of explicit tasks, such as sensory inputs and motor outputs. Spontaneous activity prevails in many brain regions and constitutes the vast majority of the total neuronal activity, and its level is little modulated by sensory inputs [6, 29]. Spontaneous activity is reported to contribute to network development [27, 47] and neural information processing [1, 15, 18, 25, 28, 36]. Thus, elucidating spontaneous activity is critical for our understanding of the brain function; however, how spontaneous activity is stably maintained or interacts with neural information are still ill defined. This is largely because it is technically difficult to manipulate spontaneous activity in the in vivo brain.

Isolated neuronal networks, such as acute brain slice preparations, also exhibit spontaneous activity [14, 21, 22, 33]. Therefore, the in vitro preparations may provide a good experimental tool to investigate the function of spontaneous activity. However, in acute slice preparations, neurites are severely cut during slicing; approximately 90 % of the axons of pyramidal neurons are pruned in 300-μm-thick neocortical slices, whereas approximately 40 % of inhibitory basket cell axons are removed [38]. Thus, in acute slices, a significant portion of the original neuronal network is destroyed, and relative intact GABAergic axons lead to dominant inhibition against glutamatergic excitation. As a result, the level of spontaneous activity is reduced in acute slices.

Organotypic slice cultures are a technique that preserves neuronal networks ex vivo [7, 39, 46]. During a course of cultivation, pruned neurites regrow and make new synaptic connections, and the network remodels itself through self-restoration. Indeed, the synaptic connectivity and the

network complexity are likely to recover to an in vivo level [42]. This natural remodeling increases the level of spontaneous activity. Thus, slice cultures have been widely used to investigate spontaneous activity [2, 34, 43]. However, no direct comparison of spontaneous activity has been conducted between ex vivo cultured networks and in vivo intact networks, and it remains unclear to what extent the frequency and patterns of spontaneous activity in ex vivo networks replicate those in in vivo networks. In the present work, we focused on hippocampal networks and evaluated the similarity of spontaneous activity among acute slices, cultured slices, and in vivo networks.

Materials and methods

Animals

Experiments were performed with the approval of the animal experiment ethics committee at the University of Tokyo (approval no. P24-6, P24-8, and P26-5) and according to the University of Tokyo guidelines for the care and use of laboratory animals. C57BL/6J mice and Wistar/ST rats (either male or female) were housed in cages under standard laboratory conditions (12 h light/dark cycle, ad libitum access to food and water). All efforts were made to minimize the animals' suffering and the number of animals used.

In vivo electrophysiology

In vivo recordings were performed using awake, head-restrained mice. Mice (postnatal day 21–27) were anesthetized with ketamine (50 mg/kg, i.p.) and xylazine (10 mg/kg, i.p.), as described elsewhere [16]. Anesthesia was confirmed by the lack of paw withdrawal, whisker movement, and eye blink reflexes. The head skin was then removed, and the animal was implanted with a metal headholding plate. After 2 days of recovery, the head-fixation training on a custom-made stereotaxic fixture was repeated for 1–3 h per day until the implanted animal learned to remain quiet. During and after each session, the animal was rewarded with ad libitum access to sucrose-containing water. During the last three sessions, sham experiments were conducted to habituate the animal to experimental conditions and noise. After full habituation, the animal was anesthetized with a ketamine/xylazine mixture. A craniotomy (1×1 mm^2), centered 2.2 mm posterior and 2.0 mm lateral to the bregma, was performed, and the dura was surgically removed. The exposed cortical surface was covered with 1.7 % agar. Throughout the experiments, a heating pad maintained the rectal temperature at 37 °C, and the surgical region was analgesized with 0.2 % lidocaine. After recovery from anesthesia, patch-clamp recordings were obtained using borosilicate glass electrodes (4–7 MΩ). Neurons in the CA1 pyramidal cell layer of the hippocampus were targeted for patch clamping. For voltage-clamped recordings, the intra-pipette solution consisted of the following (in mM): 140 Cs-methanesulfonate, 5 HEPES, 10 TEA-Cl, 1 EGTA, 10 2Na-phosphocreatine, and 1 Mg-ATP, pH 7.2, containing 0.2 % biocytin. sEPSCs and sIPSCs were obtained by maintaining the membrane potential at −70 and 0 mV, respectively. For cell-attached recordings, the patch pipettes were filled with artificial cerebrospinal fluid (aCSF) containing (in mM) 127 NaCl, 3.5 KCl, 1.24 KH_2PO_4, 1.2 $MgSO_4$, 2.0 $CaCl_2$, 26 $NaHCO_3$, and 10 glucose. The signals were amplified and digitized at a sampling rate of 20 kHz using a MultiClamp 700B amplifier and a Digidata 1440A digitizer that were controlled by pCLAMP 10.4 software (Molecular Devices). Experiments in which series resistance changed by >15 % during the entire recording session were discarded. Hippocampal pyramidal cells were electrophysiologically identified by their characteristic pattern of regular spiking and high-frequency bursts (HFBs; 100–300 Hz, 3–6 spikes) [17, 30].

Acute slice preparations

Acute slices were prepared from the medial to ventral part of the hippocampal formation as described elsewhere [22]. Mice (postnatal week 4–5) were anesthetized with ether and decapitated, and the brain was horizontally sliced (400 μm thick) at an angle of 12.7° to the fronto-occipital axis using a vibratome and an ice-cold oxygenated cutting solution consisting of (in mM) 222.1 sucrose, 27 $NaHCO_3$, 1.4 NaH_2PO_4, 2.5 KCl, 1 $CaCl_2$, 7 $MgSO_4$, and 0.5 ascorbic acid. Slices were allowed to recover for at least 1.5 h submerged in a chamber filled with oxygenated aCSF at room temperature.

Slice culture preparations

Entorhinal-hippocampal organotypic slices were prepared from postnatal day 7 Wistar/ST rats as described previously [19]. Rat pups were anesthetized by hypothermia and decapitated. The brains were removed and placed in aerated ice-cold Gey's balanced salt solution supplemented with 25 mM glucose. Horizontal entorhinal-hippocampal slices were cut at a thickness of 300 μm using a vibratome. The slices were placed on Omnipore membrane filters and incubated in 5 % CO_2 at 37 °C. The culture medium, which was composed of 50 % minimal essential medium, 25 % Hanks' balanced salt solution supplemented with 133 mM glucose, 25 % horse serum, and antibiotics, was changed every 3.5 days. Experiments were performed at 6−12 days in vitro unless otherwise specified.

In vitro electrophysiology

Recordings were performed in a submerged chamber perfused at 8 ml/min with oxygenated aCSF at 35–37 °C. Whole-cell patch-clamp recordings were obtained from hippocampal pyramidal cells visually identified under infrared differential interference contrast microscopy. Patch pipettes (3–6 MΩ) were filled with a potassium-based solution consisting of (in mM) 120 potassium gluconate, 10 KCl, 10 HEPES, 10 creatine phosphate, 4 Mg-ATP, 0.3 Na_2-GTP, and 0.2 EGTA or a cesium-based solution consisting of (in mM) 130 $CsMeSO_4$, 10 CsCl, 10 HEPES, 10 creatine phosphate, 4 Mg-ATP, and 0.3 Na_2-GTP. Spontaneous excitatory and inhibitory postsynaptic currents (EPSCs and IPSCs) were recorded at clamped voltages of −70 and 0 mV, respectively. Series resistance was not compensated.

Optical recording

For acute slices, functional multineuron calcium imaging was conducted locally loading with Oregon Green BAPTA-1AM, which can detect single spikes. Oregon Green 488 BAPTA-1AM was dissolved in DMSO containing 10 % Pluronic F-127 to yield a concentration of 200 μM. Immediately before use, this solution was diluted ten fold with aCSF and was loaded into pipettes (3–5 MΩ). The tip of the pipette was inserted into an acute hippocampal slice, and a pressure of 50–60 hPa was applied for 3–5 min using a 10-ml syringe pressurizer [22]. For cultured slices, the preparations were washed three times with oxygenated aCSF. They were transferred into a dish (35-mm diameter) containing 2 ml of the dye solution and were incubated for 1 h in a humidified incubator at 35 °C under 5 % CO_2 [13, 41]. After being washed, the cultured slices were incubated at 35 °C for 30 min and were mounted in a recording chamber perfused with aCSF at 35 °C. Fluorophores were excited at 488 nm with a laser diode and visualized using 507-nm-long pass emission filters. Videos were recorded at 50 frames/s acute slices using a 16× objective (0.8 numerical aperture, Nikon), a spinning-disk confocal microscope (CSU-X1; Yokogawa Electric, Tokyo, Japan), a cooled CCD camera (iXonEM+DV897; Andor Technology, Belfast, UK), and an upright microscope (Eclipse FN1; Nikon, Tokyo, Japan). The fluorescence change was measured as $(F_t - F_0)/F_0$, where F_t is the fluorescence intensity at time t and F_0 is the fluorescence intensity averaged from −10 to 10 s relative to t. Using principal component analysis and a support vector machine optimized to calcium imaging, spike-elicited calcium transients were semiautomatically detected with a custom-written program in Visual Basic [35].

Electrophysiological data analysis

Data were analyzed offline using custom MATLAB R2012b (The MathWorks) routines. In vivo spike activities were detected from cell-attached recording traces. After local filtering and smoothing, the monotonic-increasing fluctuations were detected, and events with amplitudes of 2–6 × SDs of the baseline noise were defined as spikes. False-positive events were removed by human operation. We counted any burst spiking at intervals of less than 300 ms as a single spike event in order to compare it with the rates of slow calcium transients. Synaptic events were detected from EPSC and IPSC traces. Events with amplitudes of 3–7 × SDs of the baseline noise after local filtering and smoothing were defined as synaptic events. To remove the possible artificial effect of high-access resistance recordings in vivo, the sEPSG amplitude was software-based corrected as described previously [44]. Then we obtained excitatory and inhibitory postsynaptic conductances (EPSGs and IPSGs) from instantaneous current amplitudes (i.e., EPSG and IPSG amplitudes, respectively) using the following potential-to-current relationship:

$$I_m = C_m\left(\frac{dV_m}{dt}\right) + g_{exc}(V_m - E_{exc}) + g_{inh}(V_m - E_{inh}) + g_{leak}(V_m - E_{leak}),$$

in which I_m represents the membrane current, C_m the membrane capacitance, V_m the membrane potential, g_{exc}/g_{inh}/g_{leak} the excitatory/inhibitory/leak conductances, and E_{exc}/E_{inh}/E_{leak} the excitatory/inhibitory/leak potential driving forces. dV_m and g_{leak} were thought to be approximated to 0. E_{inh} and E_{exc} were assumed to be −70 or 0 mV, respectively, which were clamped voltages to isolate EPSCs and IPSCs, respectively. These assumptions allowed us to calculate EPSGs and IPSGs from EPSCs and IPSCs. CV, skewness, and kurtosis were calculated from the EPSG and IPSG events.

Multidimentional scaling

We used 11 EPSGs and 14 IPSGs in vivo, 35 EPSGs and 14 IPSGs in acute slices, and 15 EPSGs and 24 IPSGs in slice cultures. The parameters (vector) of postsynaptic conductances (PSGs) consisted of the mean, coefficient of variation (CV), skewness, and kurtosis of PSG amplitude and the PSG event frequency. We calculated the Euclidean distance between each pair of vector's Z score and applied the conventional nonmetric multidimensional scaling (MDS), a dimension reduction technique for illustration purpose, to these pairwise distances. The MDS plot indicates relative pairwise distances between vectors. For the MDS results, a dendrogram was constructed using Ward's method, a hierarchical clustering algorithm. MDS and

dendrogram were calculated using MATLAB R2012b (The Mathworks) routines.

Soft confidence-weighted learning (SCW)

The SCW learning, a machine learning algorithm, consisted of two steps, i.e., the learning phase and test phase. In the learning phase, the algorithm was tuned to create the most appropriate criteria, which were later used to classify another set of preparations. More specifically, the SCW machine is exposed to the data sets of two preparations, slice cultures and acute slices (Fig. 4a, b), and in vivo preparations and acute slices (Fig. 4c, d). Each data set consisted of four parameters, i.e., the CV, skewness, and kurtosis of PSGs and the PSG event frequency. In the test phase, the trained SCW predicted (classified) a newly given data set as slice cultures or acute slices (Fig. 4a, b) and in vivo preparations or acute slices (Fig. 4c, d) based on the criteria obtained in the learning phase. All routines were written in MATLAB (The Math Works). The SCW learning code was downloaded from: http://www.cais.ntu.edu.sg/~chhoi/libol/about.html. We used the SCW-II algorithm.

Learning phase: We used 11 EPSGs and 14 IPSGs in vivo, 35 EPSGs and 14 IPSGs in acute slices, and 15 EPSGs and 24 IPSGs in slice cultures. In the classification of in vivo preparations, the SCW was exposed sequentially to individual data sets of acute and cultured slices. We used each data set that reflected the characteristic PSG parameters as a supervise vector, and each supervise vector was labeled as -1 (acute slices) or $+1$ (culture slice). During the learning, SCW gradually updated the weighted vector W, which was finally expected to be used for the most appropriate classification. Likewise, for classification of slice culture preparations, SCW was sequentially exposed to the data sets of acute slices and in vivo preparations, which are labeled as -1 or $+1$, respectively.

Test phase: SCW was newly given other data sets and was forced to judge the similarity of the preparations, based on the weighted vector W. We defined the SCW score as the relative distance from the criterion of classification as follows:

$$\text{SCW score} = W^{\mathrm{T}} x_{\mathrm{t}},$$

in which x_{t} is the data set of the preparation. The SCW score takes a positive value if the vector x_{t} is similar to cultured slices (Fig. 4a, b) or in vivo preparations (Fig. 4c, d).

Statistics

We reported the data as the mean ± SD. Median test or Kruskal-Wallis test, Mann-Whitney's U test, and Bonferroni correction were performed to assess the significance of the differences. P values <0.05 were considered statistically significant.

Results

Firing rates are similar between in vivo networks and cultured slices

Spiking activity is the major output from a neuron. If spontaneous activity in in vivo and in vitro preparations shares common information infrastructures, the spike patterns are expected to be similar. We calculated the mean firing rates of hippocampal CA1 and CA3 pyramidal cells in in vivo preparations, cultured slices, and acute slices. Spontaneous action potentials in vivo were recorded from awake mice using the cell-attached patch-clamp technique (Fig. 1a). For each cell, the activity was monitored for 2–5 min. In in vitro preparations, we recorded action potentials using functional multineuron calcium imaging in order to increase the throughput of data collection. Action potentials of a neuron evoke transient calcium increases in the cell body. The kinetics of individual calcium events are so slow that action potentials at intervals of less than 300 ms cannot be resolved in calcium traces and are captured in a single event [35]. To directly compare the in vivo and in vitro spike rates, we regarded any burst at interspike intervals of less than 300 ms as a single calcium spike. Then, we re-counted the number of total "spikes" for the entire recording period.

In acute slices and cultured slices, we recorded spontaneous firings using functional multineuron calcium imaging (Fig. 1b, c). The length of a video ranged from 2 to 10 min. For each cell, we counted the total number of individual calcium transients and calculated the "spike" rates. The mean firing rates of acute slices were $9.3 \times 10^{-6} \pm 5.5 \times 10^{-6}$ Hz (Fig. 1d; mean ± SD of 1,056 cells from 15 slices) and were significantly lower than that of cultured slices (0.048 ± 0.042 Hz of 1,178 cells from 12 slices; $P = 6.0 \times 10^{-6}$, Median test) and in vivo preparations (0.14 ± 0.21 Hz of 175 cells from 116 mice; $P = 1.0 \times 10^{-5}$). The firing rates of cultured slices were lower than those of in vivo preparations, but the difference was not statistically significant ($P = 0.38$). Note that the mean firing rates include silent cells that did not show spiking activity during our observation period. The ratios of silent cells in in vivo preparations (39 %; 68 of 175 cells) and cultured slices (38 %; 450 of 1178 cells) in cultured slices were significantly higher than those in acute slices (62 %; 658 of 1058 cells; $P = 1.2 \times 10^{-8}$ versus in vivo, $P = 2.2 \times 10^{-16}$ versus cultured slices, Fisher's exact test). These results indicate that, for the mean firing

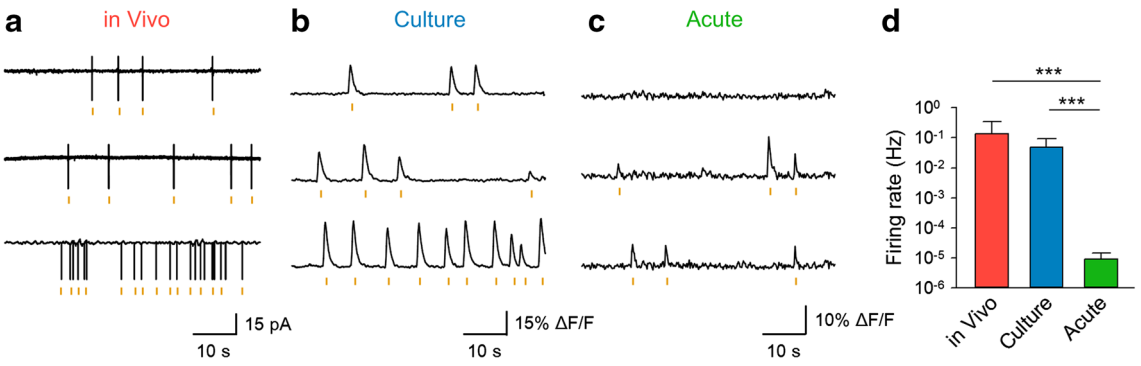

Fig. 1 Comparison of the spontaneous firing rates of CA1 neurons between the in vivo, cultured, and acute hippocampal network. Representative traces of in vivo cell-attached recording (**a**) and calcium imaging from the CA1 and CA3 pyramidal cell layer in a slice culture (**b**) and an acute slice (**c**). *Orange dots below the traces* indicate the timings of spikes. **d** The mean ± SD firing rates of 175 CA1 neurons of in vivo preparations (*red*), 1,178 neurons from 12 slice cultures (*blue*), and 1,056 neurons from 15 acute slices (*green*). ***$P < 0.001$, median test

rates, culture slices are more similar to in vivo conditions compared to acute slices.

sEPSGs are similar between in vivo networks and cultured slices

We next focused on the similarity of spontaneous synaptic activity. Using voltage-clamp recordings at −70 mV, we recorded sEPSGs from hippocampal pyramidal neurons in in vivo preparations, cultured slices, and acute slices for 1–3 min (Fig. 2a, b, c). Unlike the all-or-none fashion of spiking outputs, the intensity of synaptic inputs fluctuates continuously. For each neuron, therefore, we calculated the mean amplitude, CV, skewness, and kurtosis of its sEPSG trace (Fig. 2d). Then, data were collected from 11 cells in 11 mice (in vivo), 15 cells in 8 slice cultures, and 35 cells in 14 acute slices. The EPSG amplitude in cultured slices was 1.13 ± 0.94 nS (mean ± SD) and was significantly higher than that of in vivo preparations (0.24 ± 0.07 nS; $P = 6.0 \times 10^{-3}$, $U = 25$, Mann-Whitney's U test with Bonferroni correction after Kruskal-Wallis test) and of acute slices (0.24 ± 0.06 nS; $P = 2.70$, $U = 198$). The CV of cultured slices was 1.09 ± 0.59 and was not significantly different from that of in vivo preparations (0.82 ± 0.39; $P = 0.23$, $U = 48$). The CV of acute slices was 0.50 ± 0.23 and was significantly higher than those of in vivo preparations ($P = 9.7 \times 10^{-3}$, $U = 81$) and of slice cultures ($P = 3.4 \times 10^{-7}$, $U = 38$). Neither the skewness (in vivo: 3.95 ± 4.64, slice culture: 4.23 ± 5.29, acute slice: 2.18 ± 1.03) nor kurtosis (in vivo: 50.3 ± 103.6, slice culture: 62.1 ± 120.9, acute slice: 10.4 ± 9.0) differed among three preparations (skewness: $P = 0.73$, $\chi^2 = 0.63$; kurtosis: $P = 0.31$, $\chi^2 = 2.36$; Kruskal-Wallis test). We also detected individual EPSG events and calculated the mean event frequency (Fig. 2e). The event frequencies of in vivo preparations (10.9 ± 9.3 Hz) and cultured slices (10.5 ± 5.8 Hz) did not differ ($P = 1.0$, $U = 72$; Mann-Whitney's U test with Bonferroni correction after Kruskal-Wallis test) and were both significantly higher than those of acute slices (2.18 ± 1.93 Hz; versus slice culture: $P = 5.4 \times 10^{-4}$, $U = 55$; versus in vivo: $P = 1.8 \times 10^{-9}$, $U = 15$).

We next focused on the parameters of individual cells rather than the measurements of pooled data sets. In the above analyses, we calculated five parameters, i.e., mean, CV, skewness, kurtosis, and event frequency. Thus, the activity profile of each cell was depicted in five-dimensional space. We thus investigated the relative location of the cell's profile in the space. For illustration purposes, we first reduced the dimension of the profile using multi-dimensional scaling (MDS), based on the Z-score of pair-wise distance, which provides a visual representation of the pattern of proximities (i.e., similarities) among cells' and plotted cells' data sets in two-dimensional space (Fig. 2f). In the MDS space, the data sets of acute slices tended to be localized in a small spot, whereas those of in vivo preparations and cultured slices tended to be more widely dispersed with their data set areas overlapping each other. We analyzed these data set distributions using dendrogram-based clustering (Fig. 2g). The cells of in vivo preparations and slice cultures were ranked in an intermingled order, but the cells in acute slices tended to be more separated from the two other groups. Therefore, as a whole, sEPSCs of in vivo preparations were similar to those of slice cultures compared to those of acute slices.

sIPSGs are not similar between in vivo networks and cultured slices

We performed the same analyses for sIPSGs. sIPSGs were recorded from 14 cells in 14 mice (in vivo), 24 cells in 9 slice cultures, and 14 cells in 8 acute slices (Fig. 3a, b, c).

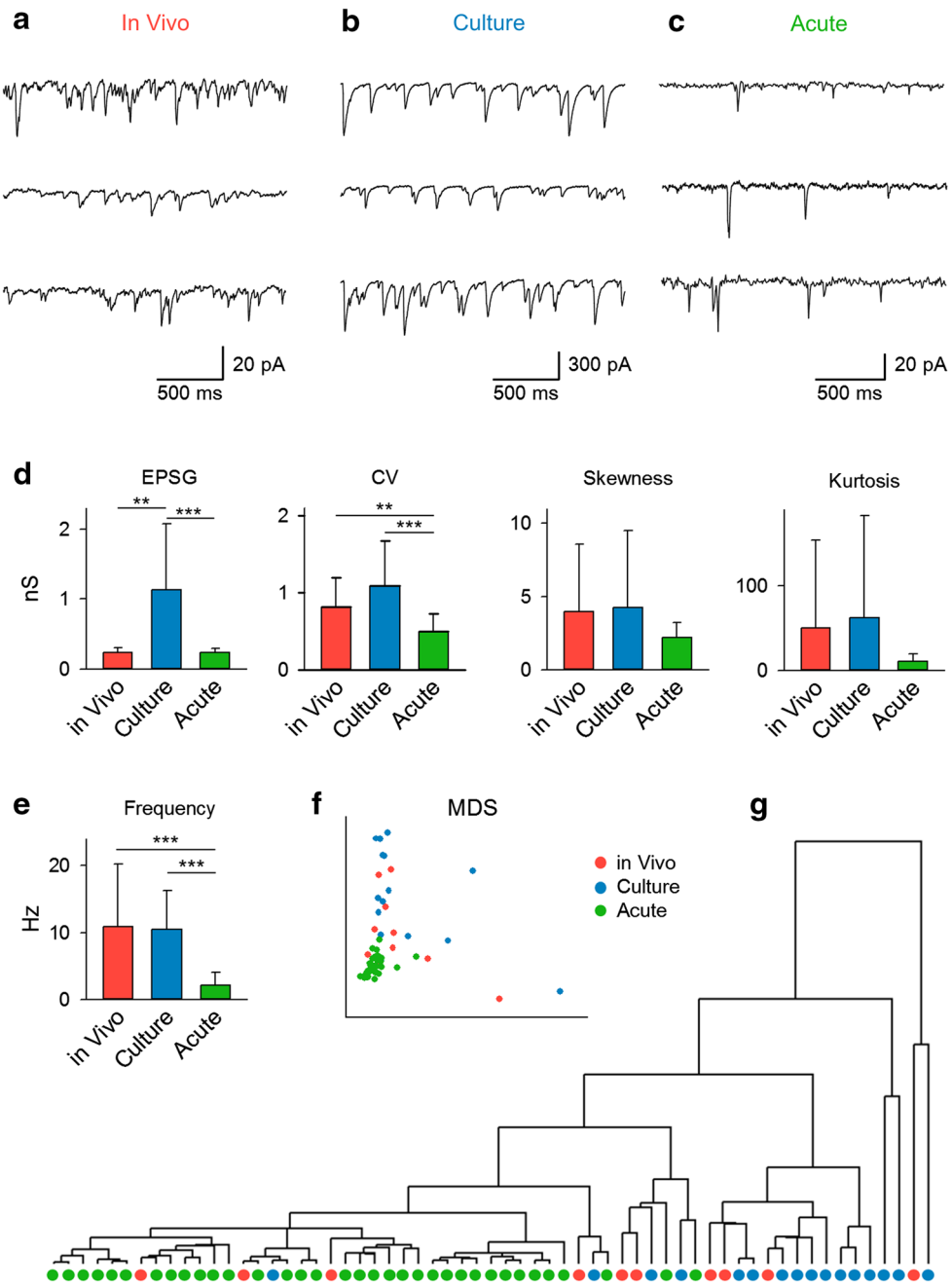

Fig. 2 Comparison of sEPSGs among in vivo, cultured, and acute hippocampal networks. Representative sEPSG traces recorded from three CA1 pyramidal neurons each in in vivo preparations (**a**), in a slice culture (**b**), and in an acute slice (**c**). **d** The mean, CV, skewness, and kurtosis of the sEPSG fluctuations are calculated for 11 cells of in vivo preparations (*red*), 15 cells of slice cultures (*blue*), and 35 cells of acute slices (*green*). $^{**}P < 0.01$, $^{***}P < 0.001$, Mann-Whitney's *U* test with Bonferroni correction. *Error bars* are SDs. **e** The frequency of sEPSG events. Data are mean ± SD of 11 cells (in vivo), 15 cells (culture), and 35 cells (acute). $^{***}P < 0.001$, Mann-Whitney's *U* test with Bonferroni correction. **f** The five parameters of individual neurons were dimension reduced to the 2D space using multidimensional scaling (MDS). Each *dot* indicates a single cell, and its color corresponds to the cohort, in vivo (*red*), slice culture (*blue*), and acute slice (*green*). The data similarity is expressed as the pairwise Euclidean distance. **g** The MDS results in **f** are classified as a dendrogram

The mean IPSG amplitude in cultured slices was 1.83 ± 0.84 nS (mean ± SD) and was significantly higher than that of in vivo preparations (Fig. 3d; 0.57 ± 0.17 nS; $P = 6.0 \times 10^{-8}$, $U = 9$, Mann-Whitney's *U* test with Bonferroni correction after Kruskal-Wallis test) and that of acute slices (1.19 ± 0.41 nS; $P = 0.017$, $U = 78$). The amplitude in acute slices was also significantly higher than that of in vivo preparations ($P = 2.8 \times 10^{-6}$, $U = 191$). The CV of sIPSGs in cultured slices was 1.02 ± 0.21 and was significantly higher than that of in vivo preparations (0.79 ± 0.25; $P = 0.013$, $U = 76$) and of acute slices (0.77 ± 0.18; $P = 3.1 \times 10^{-3}$, $U = 63$). Neither the skewness (in vivo: 2.75 ± 1.68, slice culture: 2.28 ± 0.99, acute slice: 2.58 ± 2.07) nor kurtosis (in vivo: 17.0 ± 19.0, slice culture: 11.2 ± 8.9, acute slice: 15.2 ± 22.2) differed among three preparations (skewness: $P = 0.70$, $\chi^2 = 0.71$, kurtosis: $P = 0.27$, $\chi^2 = 2.59$; Kruskal–Wallis test). The sIPSG event frequencies of in vivo preparations (11.9 ± 8.7 Hz) and cultured slices (5.59 ± 2.88 Hz) did not differ (Fig. 3e; $P = 0.12$, $U = 236$; Mann-Whitney's *U* test and Bonferroni correction after Kruskal-Wallis test) and were both significantly higher than those of acute slices

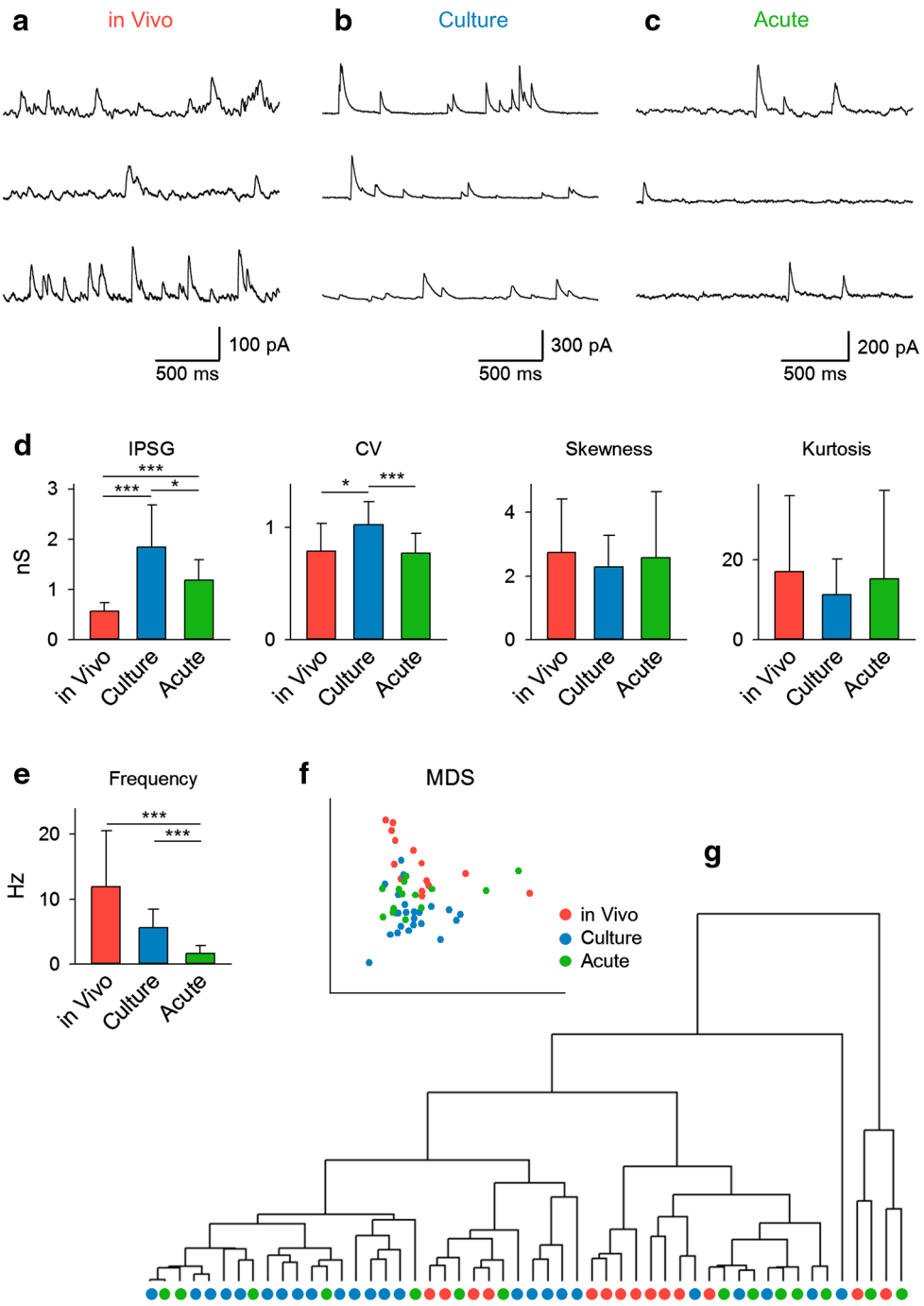

Fig. 3 Comparison of sIPSGs among in vivo, cultured, and acute hippocampal networks. Representative sIPSG traces recorded from three CA1 pyramidal neurons each in in vivo preparations (**a**), in a slice culture (**b**), and in an acute slice (**c**). **d** The mean, CV, skewness, and kurtosis of the sIPSG fluctuations are calculated for 14 cells of in vivo preparations (*red*), 24 cells of slice cultures (*blue*), and 14 cells of acute slices (*green*). $*P < 0.05$, $**P < 0.01$, $***P < 0.001$, Mann-Whitney's *U* test with Bonferroni correction. *Error bars* are SDs. **e** The mean ± SD of sIPSG event frequency. $***P < 0.001$, Mann-Whitney's *U* test with Bonferroni correction. **f** The five parameters of individual neurons were dimension reduced to the 2D space using multidimensional scaling (MDS). Each *dot* indicates a single cell, and its color corresponds to the cohort, in vivo (*red*), slice culture (*blue*), and acute slice (*green*). The data similarity is expressed as the pairwise Euclidean distance. **g** The MDS results in **f** are classified in a dendrogram

(1.64 ± 1.23 Hz; versus slice culture: $P = 1.1 \times 10^{-4}$, $U = 31$; versus in vivo: $P = 3.0 \times 10^{-4}$, $U = 19$).

Using MDS, we plotted the sIPSG data sets of individual cells in the two-dimensional space (Fig. 3f). The data sets of three groups exhibited no clear spatial separations in the MDS space. These overlapped distributions were also confirmed in the dendrogram of the MDS data (Fig. 3g). Therefore, these simple comparisons failed to indicate which is similar to in vivo preparations, slice cultures, or acute slices.

SCW classifies data sets of cultured slices as in vivo-like

The MDS algorithm has been used as an integral classification method, but it may not completely capture the net difference in the multidimensional features of synaptic activity, because MDS is designed to treat all the parameters equivalently. Therefore, we adopted the SCW learning, a recently invented supervised machine learning algorithm [45], to consider the latent difference underlying

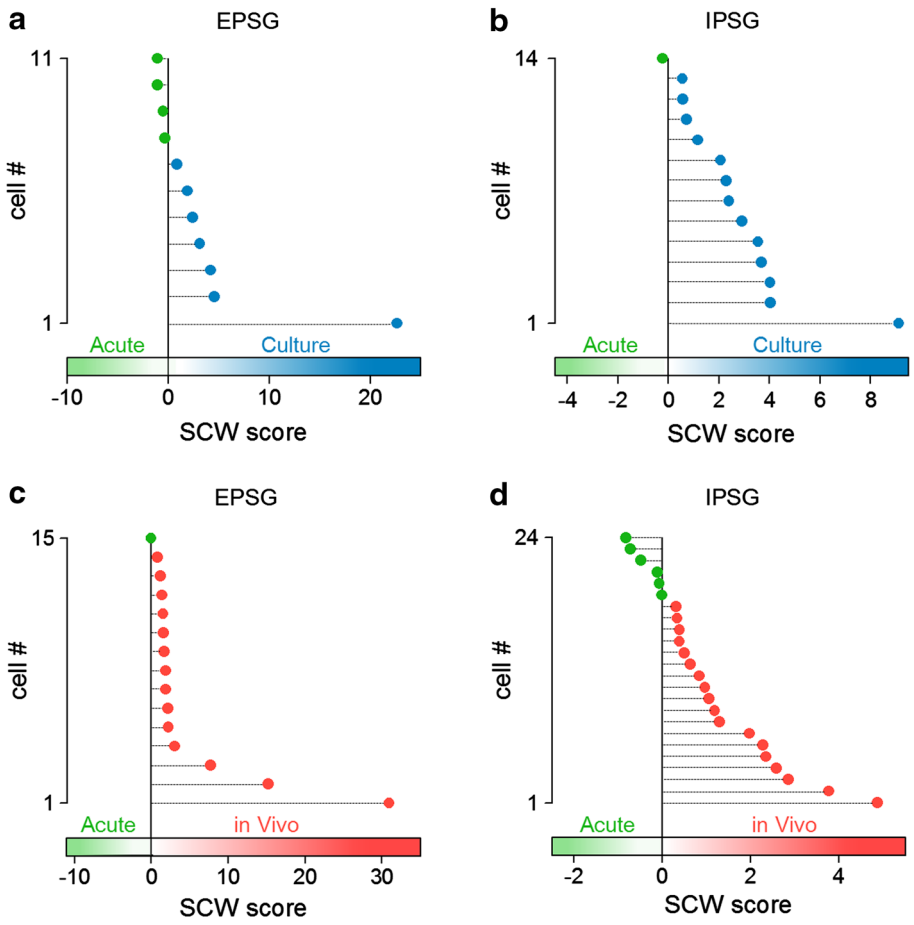

Fig. 4 SCW judged the majority of slice culture data sets as in vivo-like. **a** The *abscissa* indicates SCW scores, with higher values representing that the EPSG parameters of a given data set are more similar to those obtained from slice cultures. The ordinate indicates individual cells. The order of 11 in vivo cells was sorted along their SCW scores. SCWs judged EPSGs of 7 of the 11 in vivo cells (64 %) as slice culture-like. **b** Same as **a**, except for IPSGs. SCWs judged IPSGs in 13 of 14 in vivo cells (93 %) as slice culture-like. **c** The *abscissa* indicates SCW scores, with higher values representing that the EPSG parameters of a given data set are more similar to those obtained from in vivo recordings. The ordinate indicates individual cells. The order of the 15 cells in slice cultures was sorted along their SCW scores. SCWs judged 14 of 15 cells (93 %) as in vivo-like. **d** Same as **c**, except for IPSGs in vivo. SCWs judged IPSGs in 18 of 24 cells (75 %) as in vivo-like

the parameters of synaptic activity without any human bias, because SCW can estimate the features of skewness and kurtosis in each cell even when the parameters are largely distributed.

For sEPSGs and sIPSGs, SCW was exposed sequentially to individual data sets of slice cultures and acute slices, which consisted of the CV, skewness, kurtosis of PSGs, and the PSGs event frequency. Based on these parameters, SCW gradually calculated a weight vector during this learning phase and thereby learned the overall parameter tendencies of slice cultures and acute slices. We defined the dot product of the weight vector and data set parameters as the SCW score; a more positive SCW score indicates a higher similarity to slice cultures. After the learning phase, we obtained the SCW score of each in vivo data set by inputting its parameters to the trained SCW (test phase). In other words, the trained SCW was asked to judge whether a given in vivo data set is more "slice culture-like" or "acute slice-like" based on its prior knowledge about the parameter tendencies of slice cultures and acute slices.

For the sEPSG data sets of in vivo preparations, SCWs gave positive SCW scores in 7 of the 11 in vivo cells (64 %), that is, more than a half of the in vivo cells were judged to be more similar to slice-cultured cells rather than acute-slice cells (Fig. 4a). For the sIPSG data sets, SCWs concluded that 13 of 14 cells (93 %) were more similar to slice-cultured cells (Fig. 4b). These results suggest that in vivo preparations and slice cultures are similar in both EPSGs and IPSGs.

To further confirm this tendency, we next trained the SCW machine using the data sets of in vivo preparations and acute slices (learning phase) and asked it whether individual data sets of slice cultures are more similar to those in the parameters of in vivo preparations or acute slices (test phase). For the sEPSG data sets of slice cultures, SCWs judged 14 of 15 cells (93 %) as in vivo cell-like rather than acute-slice cell-like (Fig. 4c). For the sIPSG data sets, SCWs concluded that 18 of 24 cells (75 %) were more similar to in vivo cells (Fig. 4d).

Discussion

In this work, we compared spontaneous activity of hippocampal neurons among acute slices, cultured slices, and in vivo networks and found that, as a whole, spontaneous

activity of slice cultures was more similar to that of in vivo preparations in terms of both spike outputs and synaptic inputs. Therefore, cultured slices are suggested to be a useful tool for investigating spontaneous network activity.

We used mice for in vivo preparations and acute slices, whereas we used rats for slice cultures. This is simply due to the routine experimental systems of our laboratory. We do not think that different species affected our results, because the spontaneous activity level in the hippocampus is almost equivalent between rats and mice; the mean firing rate of rat hippocampal neurons is reported to be about 0.27 Hz during quiet awake states [26] and does not differ from the in vivo firing rate in our head-restricted mouse (0.14 ± 0.21 Hz). One of the remarkable differences between in vivo and in vitro preparations is that in vivo animals drift across different brain states, including actively exploring, resting, and sleeping states. The firing rates of neurons and the oscillation powers of local field potentials change depending on these behavioral states [3, 26]. We fixed the head of the mice to a stereotaxic frame; thus, we expected that the mice spent the majority of their time for quite awake or sleep. However, we cannot strictly determine which in vivo state corresponded to the spontaneous state of our in vitro preparations. Nonetheless, it is notable that in vivo data were still similar to cultured slice data even when all in vivo data were blindly pooled irrespective of their states. On the other hand, we leave open the question of whether some aspect in the activity of acute slices may represent a specific state of in vivo animals more faithfully.

The mean firing rates are thought to represent an aspect of information coding [9, 31, 37]. The similarity of the mean firing rates between in vivo preparations and slice cultures suggest that these preparations share a common circuit basis for spontaneous spiking. During cultivation, slice cultures restore the complexity of their neuronal network through neuritogenesis and synaptogenesis. This self-organization process occurs spontaneously depending on the intrinsic network formation rules; note that slice cultures do not receive sensory inputs and thus mature purely through their own activity and the inherent laws. Our data indicate that such spontaneously emerging networks can behave like in vivo networks. Thus, cultivation ameliorates artificially damaged networks in acute slices. This idea is consistent with a previous report showing that the difference of evoked unitary synaptic activity in monosynaptically connected neuron pairs between cultured and acute hippocampus slices depends on the density of synaptic connections [5]; the CA3-CA1 excitatory connection probability is 76 % in slice cultures and 6 % in acute slices, and the CA3-CA3 connection probability is 56 % in slice cultures and 1.5 % in acute slices. However, these data must be interpreted with caution, because the circuit density is subject to developmental changes during cultivation. Indeed, the amplitudes of evoked EPSPs are known to change as a function of days in vitro [12, 23]. In the present work, we used slice cultures after 6–12 days in vitro. Evaluations using electrophysiology and morphology demonstrate that the developmental maturation of hippocampal neurons under cultured conditions is almost equivalent to day-matched neurons in vivo [4]. Based on this calculation, our slice cultures are estimated to correspond to the neural conditions in 13-to-19-day-old mice. In general, cortical neurons generate widely synchronized activity during early development [24], and the activity patterns become more decorrelated in the course of neuronal network maturation [10, 32]. After that, the firing rates are kept almost constant over long postnatal days [20]. We believe that all our preparations already reached the final stage of maturation, because their spiking activity was rather sparse.

The high-order sEPSG kinetics parameters, such as CV, skewness, and kurtosis, reflect neuronal synchronization. Synchronized synaptic inputs come from the population activity of presynaptic cell ensembles and cause large membrane potential fluctuations [8, 40]. The fact that these parameters were similar between in vivo preparations and slice cultures suggests that the entire network activity patterns are also organized in a similar manner. On the other hand, the sIPSG parameters were not necessarily similar between in vivo preparations and slice cultures and did not differentiate in the MDS space. A possible explanation is that the axons of GABAergic interneurons are more spared after slicing relative to those of pyramidal cells [38], because hippocampal GABAergic neurons tend to innervate nearby neurons [11]. Therefore, compared to excitatory synaptic activity, spontaneous inhibitory activity may not be severely reduced in acute slices. However, SCW separated IPSGs in acute slices from those of in vivo parameters and slice cultures. Given that firings of inhibitory neurons are driven by excitatory inputs, we believe spontaneous inhibitory activity is also affected in acute slices even though their network per se is relatively intact.

Acknowledgments We are grateful to Dr. Hiroshi Ban (CiNET) for his technical support for soft confidence weighted. This work was supported by Kakenhi (22115003; 26250003; 25119004).

Conflict of interest The authors declare no competing financial interests.

References

1. Arieli A, Sterkin A, Grinvald A, Aertsen A (1996) Dynamics of ongoing activity: explanation of the large variability in evoked cortical responses. Science 273:1868–1871
2. Beggs JM, Plenz D (2003) Neuronal avalanches in neocortical circuits. J Neurosci 23:11167–11177

3. Buzsaki G, Leung LW, Vanderwolf CH (1983) Cellular bases of hippocampal EEG in the behaving rat. Brain Res 287:139–171
4. De Simoni A, Griesinger CB, Edwards FA (2003) Development of rat CA1 neurones in acute versus organotypic slices: role of experience in synaptic morphology and activity. J Physiol 550:135–147
5. Debanne D, Guerineau NC, Gahwiler BH, Thompson SM (1995) Physiology and pharmacology of unitary synaptic connections between pairs of cells in areas CA3 and CA1 of rat hippocampal slice cultures. J Neurophysiol 73:1282–1294
6. Fiser J, Chiu C, Weliky M (2004) Small modulation of ongoing cortical dynamics by sensory input during natural vision. Nature 431:573–578
7. Gahwiler BH, Capogna M, Debanne D, McKinney RA, Thompson SM (1997) Organotypic slice cultures: a technique has come of age. Trends Neurosci 20:471–477
8. Gasparini S, Magee JC (2006) State-dependent dendritic computation in hippocampal CA1 pyramidal neurons. J Neurosci 26:2088–2100
9. Geisler WS, Albrecht DG, Salvi RJ, Saunders SS (1991) Discrimination performance of single neurons: rate and temporal-pattern information. J Neurophysiol 66:334–362
10. Golshani P, Goncalves JT, Khoshkhoo S, Mostany R, Smirnakis S, Portera-Cailliau C (2009) Internally mediated developmental desynchronization of neocortical network activity. J Neurosci 29:10890–10899
11. Gulyas AI, Miles R, Hajos N, Freund TF (1993) Precision and variability in postsynaptic target selection of inhibitory cells in the hippocampal CA3 region. Eur J Neurosci 5:1729–1751
12. Ikegaya Y (1999) Abnormal targeting of developing hippocampal mossy fibers after epileptiform activities via L-type Ca2+ channel activation in vitro. J Neurosci 19:802–812
13. Ikegaya Y, Le Bon-Jego M, Yuste R (2005) Large-scale imaging of cortical network activity with calcium indicators. Neurosci Res 52:132–138
14. Ikegaya Y, Aaron G, Cossart R, Aronov D, Lampl I, Ferster D, Yuste R (2004) Synfire chains and cortical songs: temporal modules of cortical activity. Science 304:559–564
15. Ikegaya Y, Sasaki T, Ishikawa D, Honma N, Tao K, Takahashi N, Minamisawa G, Ujita S, Matsuki N (2012) Interpyramid spike transmission stabilizes the sparseness of recurrent network activity. Cereb Cortex.
16. Ishikawa D, Matsumoto N, Sakaguchi T, Matsuki N, Ikegaya Y (2014) Operant conditioning of synaptic and spiking activity patterns in single hippocampal neurons. J Neurosci 34:5044–5053
17. Kandel ER, Spencer WA (1961) Electrophysiology of hippocampal neurons. II. After-potentials and repetitive firing. J Neurophysiol 24:243–259
18. Kenet T, Bibitchkov D, Tsodyks M, Grinvald A, Arieli A (2003) Spontaneously emerging cortical representations of visual attributes. Nature 425:954–956
19. Koyama R, Muramatsu R, Sasaki T, Kimura R, Ueyama C, Tamura M, Tamura N, Ichikawa J, Takahashi N, Usami A, Yamada MK, Matsuki N, Ikegaya Y (2007) A low-cost method for brain slice cultures. J Pharmacol Sci 104:191–194
20. Langston RF, Ainge JA, Couey JJ, Canto CB, Bjerknes TL, Witter MP, Moser EI, Moser MB (2010) Development of the spatial representation system in the rat. Science 328:1576–1580
21. Mao BQ, Hamzei-Sichani F, Aronov D, Froemke RC, Yuste R (2001) Dynamics of spontaneous activity in neocortical slices. Neuron 32:883–898
22. Mizunuma M, Norimoto H, Tao K, Egawa T, Hanaoka K, Sakaguchi T, Hioki H, Kaneko T, Yamaguchi S, Nagano T, Matsuki N, Ikegaya Y (2014) Unbalanced excitability underlies offline reactivation of behaviorally activated neurons. Nat Neurosci 17:503–505
23. Muller D, Buchs PA, Stoppini L (1993) Time course of synaptic development in hippocampal organotypic cultures. Brain Res Dev Brain Res 71:93–100
24. Namiki S, Norimoto H, Kobayashi C, Nakatani K, Matsuki N, Ikegaya Y (2013) Layer III neurons control synchronized waves in the immature cerebral cortex. J Neurosci 33:987–1001
25. Pare D, Shink E, Gaudreau H, Destexhe A, Lang EJ (1998) Impact of spontaneous synaptic activity on the resting properties of cat neocortical pyramidal neurons In vivo. J Neurophysiol 79:1450–1460
26. Pavlides C, Winson J (1989) Influences of hippocampal place cell firing in the awake state on the activity of these cells during subsequent sleep episodes. J Neurosci 9:2907–2918
27. Penn AA, Shatz CJ (1999) Brain waves and brain wiring: the role of endogenous and sensory-driven neural activity in development. Pediatr Res 45:447–458
28. Petersen CC, Hahn TT, Mehta M, Grinvald A, Sakmann B (2003) Interaction of sensory responses with spontaneous depolarization in layer 2/3 barrel cortex. Proc Natl Acad Sci USA 100:13638–13643
29. Raichle ME (2006) Neuroscience. The brain's dark energy. Science 314:1249–1250
30. Ranck JB Jr (1973) Studies on single neurons in dorsal hippocampal formation and septum in unrestrained rats. I. Behavioral correlates and firing repertoires. Exp Neurol 41:461–531
31. Redman SJ, Lampard DG, Annal P (1968) Monosynaptic stochastic stimulation of cat spinal motoneurons. II. Frequency transfer characteristics of tonically discharging motoneurons. J Neurophysiol 31:499–508
32. Rochefort NL, Garaschuk O, Milos RI, Narushima M, Marandi N, Pichler B, Kovalchuk Y, Konnerth A (2009) Sparsification of neuronal activity in the visual cortex at eye-opening. Proc Natl Acad Sci USA 106:15049–15054
33. Sanchez-Vives MV, McCormick DA (2000) Cellular and network mechanisms of rhythmic recurrent activity in neocortex. Nat Neurosci 3:1027–1034
34. Sasaki T, Matsuki N, Ikegaya Y (2007) Metastability of active CA3 networks. J Neurosci 27:517–528
35. Sasaki T, Takahashi N, Matsuki N, Ikegaya Y (2008) Fast and accurate detection of action potentials from somatic calcium fluctuations. J Neurophysiol 100:1668–1676
36. Shu Y, Hasenstaub A, Badoual M, Bal T, McCormick DA (2003) Barrages of synaptic activity control the gain and sensitivity of cortical neurons. J Neurosci 23:10388–10401
37. Softky WR (1995) Simple codes versus efficient codes. Curr Opin Neurobiol 5:239–247
38. Stepanyants A, Martinez LM, Ferecsko AS, Kisvarday ZF (2009) The fractions of short- and long-range connections in the visual cortex. Proc Natl Acad Sci U S A 106:3555–3560
39. Stoppini L, Buchs PA, Muller D (1991) A simple method for organotypic cultures of nervous tissue. J Neurosci Methods 37:173–182
40. Stuart G, Schiller J, Sakmann B (1997) Action potential initiation and propagation in rat neocortical pyramidal neurons. J Physiol 505(Pt 3):617–632
41. Takahashi N, Sasaki T, Usami A, Matsuki N, Ikegaya Y (2007) Watching neuronal circuit dynamics through functional multineuron calcium imaging (fMCI). Neurosci Res 58:219–225
42. Takahashi N, Sasaki T, Matsumoto W, Matsuki N, Ikegaya Y (2010) Circuit topology for synchronizing neurons in spontaneously active networks. Proc Natl Acad Sci U S A 107:10244–10249
43. Takahashi N, Kitamura K, Matsuo N, Mayford M, Kano M, Matsuki N, Ikegaya Y (2012) Locally synchronized synaptic inputs. Science 335:353–356
44. Traynelis SF (1998) Software-based correction of single compartment series resistance errors. J Neurosci Methods 86:25–34

45. Wang J, Zhao P, Hoi SCH (2012) Exact soft confidence-weighted learning. Int Conf Mach Learn Proc 1206:4612
46. Yamamoto N, Kurotani T, Toyama K (1989) Neural connections between the lateral geniculate nucleus and visual cortex in vitro. Science 245:192–194
47. Zhang LI, Poo MM (2001) Electrical activity and development of neural circuits. Nat Neurosci 4:1207–1214